Article

Theoretical Study on Structure and Sum-Frequency Generation (SFG) Spectroscopy of Styrene−Graphene Adsorption System

Chih-Kai Lin,*,[†,‡] Chun-Chi Shih,[†] Yingli Niu,[†] Min-Yeh Tsai,[†] Ying-Jen Shiu,[†,‡] Chaoyuan Zhu,[†] Michitoshi Hayashi,[§] and Sheng Hsien Lin[†,‡]

[†]Department of Applied Chemistry, National Chiao Tung University, Hsinchu, Taiwan 30010, ROC
[‡]Institute of Atomic and Molecular Sciences, Academia Sinica, Taipei, Taiwan 10617, ROC
[§]Center for Condensed Matter Sciences, National Taiwan University, Taipei, Taiwan 106, ROC

ABSTRACT: In this theoretical study, we aimed to simulate the sum-frequency generation (SFG) spectroscopy of a thin polystyrene layer physically adsorbed on the graphene sheet and to figure out the orientation distribution of the phenyl units. To simplify the problem, we started the investigation by constructing molecular models with styrene and ethylbenzene monomers and styrene oligomers up to four units adsorbed on a finite-sized graphene hexagon. Geometric optimization results showed that the phenyl rings of the adsorbate always orientate close to the surface normal with a small tilt angle. The adsorption is weak but not negligible. SFG spectra have been simulated based on these calculated structures, vibrational frequencies, and dipole and polarizability derivatives to compare with experimental reports of polystyrene adsorbed on other surfaces.
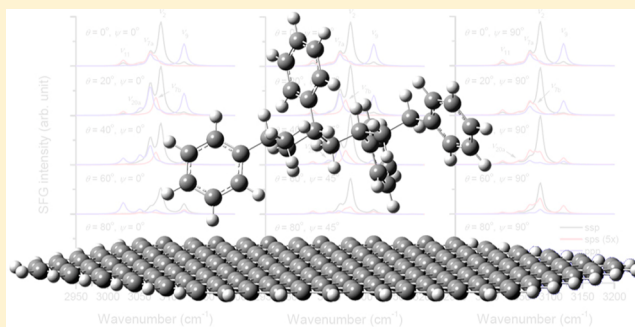
I. INTRODUCTION

The sum-frequency generation (SFG) spectroscopy has in recent years become a powerful technique to survey the surface or interface conformation of condensed materials. The achievement is attributed to its nonlinear optical character; that is, the spatial average of the second-order susceptibility, $\chi^{(2)}$, does not vanish in a noncentrosymmetric system.[1−4] On the surface or interface of materials, 7 of the 27 components in the third-rank tensor $\chi^{(2)}$ survive. The peak intensities obtained from the SFG spectrum are then determined by the incident light beams as well as the spatial-averaged magnitude of these tensor components, which in turn are affected by the orientation of surface/interface molecules.

The SFG spectroscopy, in principle, can be achieved by using any combination of two incident light beams. In practice, the resonance−off-resonance setting is mostly applied where the first (infrared) beam is tuned on resonance with a certain vibrational level of the molecular system, and the second (visible or ultraviolet) beam excites the system to a virtual electronic state. A resulted output beam with the sum frequency is then recorded when the incident beams are carefully arranged. By scanning the vibrational part and recording the output signals, a profile of surface or interface conformation would emerge. This technique has been successfully applied in studying configurations of the liquid water−vapor interface,[5−7] the ice surface,[2] organic adsorbate−substrate interfaces[8−11] as well as chiral compounds[4] and protein secondary structural motifs.[12]

When a polymer molecule with side groups is adsorbed on a certain solid substrate, the orientations of these side groups should be determined by interactions between monomer units and between polymer molecule and substrate as well as the potential of free groups toward the air (or the vacuum). In case the adsorbed polymer film is thick enough, the configuration at the bottom (near the polymer−substrate interface) is expected different from that at the top (the polymer surface). People have explored, for example, the polystyrene (PS) film coated on solids and analyzed their SFG spectra to identify the tilt angle of the phenyl rings. Gautam et al. reported that the tilt angle was ∼20° at the PS/air interface and ∼70° at the PS/sapphire interface where the PS film had a thickness of 160 nm.[8] Briggman et al. suggested that, however, the angle was near 57° at the free surface in a PS−silicon system and in addition the phenyl groups on the surface were ordered and orientated outward.[9] In a more recent experiment, Han and Shen studied the PS−graphene system with SFG spectroscopy, yet they could not obtain a solid conclusion whether the phenyl groups tend to orientate to the surface normal or to tilt away.[13]

In this theoretical work, we attempted to find out the most stable conformations of the styrene−graphene system and to simulate the SFG spectra. To simplify the problem, we made a systematic investigation starting from styrene monomer and ethylbenzene molecule adsorbed on a graphene sheet and then

Table 1. Comparison of Phenyl and Vinyl C−H Stretching Mode Frequencies (in cm^{-1}, calibrated by a common scaling factor for all modes in each calculation according to Refs 15 and 16) of Styrene Monomer Calculated at Different Levels of Theory and Basis Sets

mode[a]		vinyl		phenyl						vinyl
		ν_{11}	ν_1	ν_{20a}	ν_{7b}	ν_{7a}	ν_{20b}	ν_2		ν_9
HF/6-31G		2997	3016	3023	3030	3041	3052	3062		3086
HF/6-31G(d)		2992	3007	3012	3018	3029	3039	3047		3073
B3LYP/6-31G		3032	3054	3065	3072	3082	3092	3102		3133
B3LYP/6-31G(d)		3024	3046	3050	3056	3066	3074	3082		3119
B3LYP/6-31+G(d,p)		3031	3046	3057	3064	3073	3082	3089		3125
B3LYP/6-311+G(3df,2p)		3025	3039	3050	3057	3067	3076	3084		3114
B3LYP/aug-cc-pVDZ		3049	3059	3073	3080	3089	3099	3105		3143
PBEPBE/6-31G		3041	3065	3076	3083	3094	3103	3116		3151
PBEPBE/6-31G(d)		3034	3058	3062	3070	3079	3087	3097		3137
expt.	IR[b]	2982	3010	3029		3061	3084	3090		3105
	Raman[b]	2981	3009		3055	3061		3091		3107
	Raman[a]	2983	3011	3011		3059	3066			3093

[a]Assignments and data from ref 18. [b]Ref 22.

step-by-step increasing the adsorbate size up to styrene tetramer. Several different conformations of these monomers and oligomers have been tested, showing that the phenyl rings tend to stick up from the graphene surface rather than to lay parallel to it. Calculated stable structures and simulated SFG spectra are illustrated in the following sections.

II. THEORIES

The theoretical framework of SFG vibrational spectroscopy has been well developed, and here we followed Shen's formalism.[2] Given the angular frequencies of SFG, visible, and infrared beams as ω_{SFG}, ω_{Vis}, and ω_{IR}, respectively, the second-order susceptibility of a group of molecules under the resonance−off-resonance SFG scheme can be expressed as

$$\chi^{(2)}(-\omega_{SFG}; \omega_{Vis}, \omega_{IR}) = \chi^{(2)}_{NR} + \chi^{(2)}_R \tag{1}$$

$$\chi^{(2)}_R = \sum_q \frac{A_{q,IJK}}{\omega_{IR} - \omega_q + i\Gamma_q} \tag{2}$$

where $\chi^{(2)}_{NR}$ and $\chi^{(2)}_R$ are the nonresonant background and the resonant contribution, respectively. $A_{q,IJK}$, ω_q, and Γ_q are the macroscopic amplitude, vibrational frequency, and damping constant of the qth vibrational mode, respectively, with I, J, and K indicating the laboratory frames X, Y, and Z. The resonant part is expected to be dominant when the system is fully or nearly on resonance. The relationship between the macroscopic amplitude of a group of randomly oriented molecules and the microscopic amplitude of a single molecule is

$$A_{q,IJK} = N \sum_{lmn} a_{q,lmn} \langle (\hat{I}\cdot\hat{l})(\hat{J}\cdot\hat{m})(\hat{K}\cdot\hat{n}) \rangle$$
$$= N \sum_{lmn} a_{q,lmn} \langle R_{Il} R_{Jm} R_{Kn} \rangle \tag{3}$$

where l, m, and n refer to molecular coordinates x, y, and z, N is the density of molecules at the interface, and $\langle \cdots \rangle$ is the orientation average. The nine components of the rotation matrix for the Euler angle transformation, that is, R_{Xx}, R_{Xy}, R_{Xz}, and so on, have been elucidated following a z-y-z convention in the literature.[3] The microscopic amplitude is further related to the dipole derivative, $\partial\mu/\partial Q_q$, and the polarizability derivative, $\partial\alpha/\partial Q_q$, through the equation

$$a_{q,lmn} = -\frac{1}{2\varepsilon_0\omega_q} \frac{\partial\mu_n}{\partial Q_q} \frac{\partial\alpha_{lm}}{\partial Q_q} \tag{4}$$

where Q_q is the qth normal mode coordinate.

Now take an instrumental setup that the incident angles of the visible and the infrared beams are θ_{Vis} and θ_{IR}, respectively, and the output angle of the sum-frequency beam is θ_{SFG} with respect to the surface normal. Considering the polarization of beams (s or p) and Fresnel factors (L), the effective macroscopic amplitudes that can be detected are[2]

$$A_{q,eff}(ssp) = \sin\theta_{IR} L_{YY}(\omega_{SFG}) L_{YY}(\omega_{Vis}) L_{ZZ}(\omega_{IR}) A_{q,XXZ} \tag{5}$$

$$A_{q,eff}(sps) = \sin\theta_{Vis} L_{YY}(\omega_{SFG}) L_{ZZ}(\omega_{Vis}) L_{YY}(\omega_{IR}) A_{q,XZX} \tag{6}$$

$$A_{q,eff}(ppp) = \sin\theta_{SFG} \sin\theta_{Vis} \sin\theta_{IR} L_{ZZ}(\omega_{SFG}) L_{ZZ}(\omega_{Vis}) L_{ZZ}(\omega_{IR}) A_{q,ZZZ}$$
$$- \cos\theta_{SFG} \cos\theta_{Vis} \sin\theta_{IR} L_{XX}(\omega_{SFG}) L_{XX}(\omega_{Vis}) L_{ZZ}(\omega_{IR}) A_{q,XXZ}$$
$$+ \sin\theta_{SFG} \cos\theta_{Vis} \cos\theta_{IR} L_{ZZ}(\omega_{SFG}) L_{XX}(\omega_{Vis}) L_{XX}(\omega_{IR}) A_{q,ZXX}$$
$$- \cos\theta_{SFG} \sin\theta_{Vis} \cos\theta_{IR} L_{XX}(\omega_{SFG}) L_{ZZ}(\omega_{Vis}) L_{XX}(\omega_{IR}) A_{q,XZX} \tag{7}$$

where the sequence of beam polarization noted here is SFG, visible, and infrared. On a surface where the adsorbates have a random azimuthal distribution, only seven elements of the second-order susceptibility tensor survive, and some of them are mutually dependent after the orientation average:

$$A_{q,ZZZ}, A_{q,XXZ} = A_{q,YYZ}, A_{q,ZXX} = A_{q,XZX} = A_{q,ZYY}$$
$$= A_{q,YZY} \tag{8}$$

and according to eqs 5 and 6, the relative intensities of different vibrational modes in ssp or sps spectra are not affected by incident angles because $\sin\theta_{Vis}$ or $\sin\theta_{IR}$ is just a common factor. The ppp signals, in contrast, will change its peak-to-peak ratios when the beam angles change.

III. COMPUTATIONAL DETAILS

Model molecular systems composed of graphene sheet and adsorbates were constructed to investigate their IR, Raman, and SFG properties in this work. A finite-sized hexagonal graphene sheet composed of up to 216 carbon atoms was constructed,

where the edges were passivated by hydrogen atoms and the sheet size was large enough to avoid interaction between the edge and adsorbates. Tested adsorbates including styrene monomer, (polymerized) dimer, trimer, and tetramer were then placed above the center of the graphene sheet. The ethylbenzene molecule, which is the single-bond analogue to the styrene monomer, was also studied.

All of these model systems were geometrically optimized with the graphene sheet frozen. It was followed by calculations of IR and Raman components and their derivatives, which yielded the second-order susceptibility, $\chi^{(2)}$, for generating SFG spectra. HF and DFT computations with some functionals and basis sets were carried out, among which B3LYP/6-31G(d) showed a relatively good performance (see Table 1 and following discussion). All computations were done by using the Gaussian 09 package,[14] where $\partial\mu_n/\partial Q_q$ and $\partial\alpha_{lm}/\partial Q_q$ were calculated using the keyword IOP(7/33=1) implemented therein.

IV. RESULTS AND DISCUSSION

1. Spectra of Styrene Monomer and Oligomers. *IR and Raman Spectra.* The SFG amplitude is directly related to the dipole derivative and the polarizability derivative (eq 4), and hence the IR and Raman spectra can be the first touchstone to the correctness of computed results. For styrene monomer, vibrational frequencies of C−H stretching modes have been calculated by using different levels of theory and basis sets as listed in Table 1, where the values have been calibrated by scaling factors from literature.[15,16] Simulated IR and Raman spectra at the high-frequency region are illustrated in Figure 1,
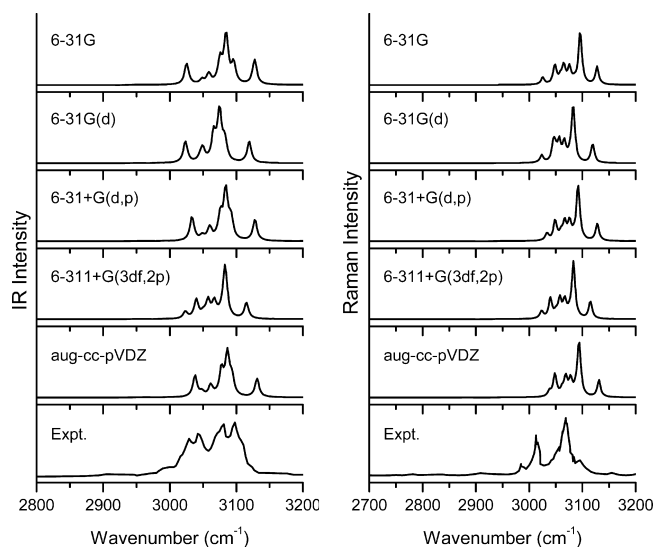

Figure 1. Simulated IR and Raman spectra of styrene monomer in the C−H stretching mode region calculated by B3LYP with different basis sets. Experimental IR and Raman spectra were adopted from refs 17 and 18, respectively. The intensity was normalized to the highest peak in each panel.

together with experimental reports for comparison.[17,18] Among these results, the B3LYP functional with 6-31+G(d,p) yielded quite accurate vibrational frequencies and spectral shape, which could get little improvement by further enlarging the basis set. B3LYP/6-31G(d) gave a moderate balance between accuracy on frequencies (with a common scaling factor of 0.960) and

computational consumption and hence were widely applied in this work.

There are eight C−H stretching modes ranging from 2980 to 3150 cm^{-1} for styrene monomer, among which the lowest two and the highest one belong to the vinyl group whereas the other five belong to the phenyl group. By careful comparison between calculated and experimental spectral peaks, the five phenyl modes, ν_2, ν_{20b}, ν_{7a}, ν_{7b}, and ν_{20a}, were assigned in descending frequency. The vibrational motions of these modes are depicted in Figure 2 after Varsányi.[19,20] It should be noticed
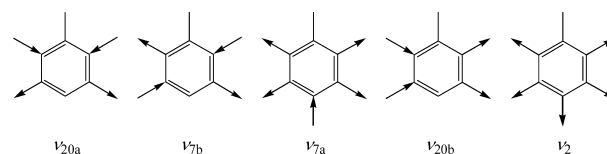

Figure 2. Phenyl C−H stretching modes of the styrene monomer.

that in our calculations ν_2 always had the highest frequency among the five modes, which has been reported by Briggman et al.[9] but was inconsistent with experimental assignments.[8,18] ν_{20b} was higher than ν_{20a} and ν_{7a} was higher than ν_{7b}, respectively, which followed experiments deduced by Sears et al.[18] but were in contrast with a previous SFG assignment.[8]

For (polymerized) styrene dimers, trimers, and tetramers, there are numerous possible conformers attributed to the freely rotating C−C backbone. We have searched some stable conformers for each oligomer and found that, in general, the IR and Raman spectra had insignificant differences between each other. The spectra of most stable conformers are illustrated in Figure 3, and the corresponding phenyl C−H stretching peaks are listed in Table 2. Comparing their IR spectra to styrene monomer (cf. Figure 1), the highest vinyl mode above 3100 cm^{-1} vanished, whereas many alkyl modes appeared under 3000 cm^{-1}. However, the IR spectra of these oligomers were not close enough to the experimental polymer at the first glance (cf. Figure 3). One possible reason is that a
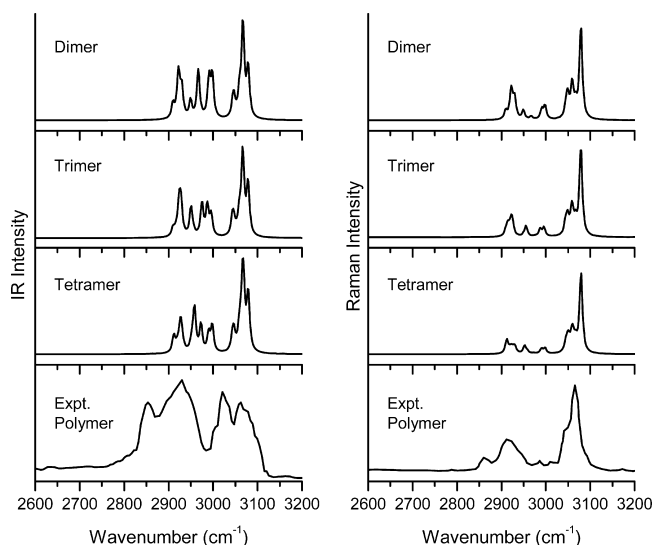

Figure 3. Simulated IR and Raman spectra of styrene oligomers in the C−H stretching mode region calculated by B3LYP/6-31G(d). Experimental IR and Raman spectra were adopted from refs 21 and 18, respectively. The intensity was normalized to the highest peak in each panel.

Table 2. Comparison of Phenyl C−H Stretching Mode Frequencies (in cm^{-1}, calibrated by a common scaling factor of 0.960) of Styrene Monomer and Oligomers Calculated by B3LYP/6-31G(d)

mode		ν_{20a}	ν_{7b}	ν_{7a}	ν_{20b}	ν_2
ethylbenzene		3041	3053	3063	3075	3083
styrene monomer		3050	3056	3066	3074	3082
styrene dimer		3044−3046	3047−3050	3059−3060	3066−3068	3078−3079
styrene trimer		3041−3047	3046−3053	3057−3061	3066−3068	3078−3079
styrene tetramer		3042−3046	3047−3053	3058−3062	3066−3069	3078−3080
styrene polymer, expt.	IR[a]	3027			3060	3083
	Raman[a]		3034	3050	3060	
	Raman[b]	3007		3058	3067	

[a]Ref 9. [b]Ref 22.

real polymer sample has countless alkyl C−H modes that may cause a broad band. Meanwhile, we noticed that the experimental resolution was not good so the comparison might become less valuable.[21] The Raman spectra showed a good resemblance between calculated oligomers and experimental polymer, indicating that our calculation was reliable.[9,18,22]

SFG Spectra. According to the Euler angle transformation, the orientation of the adsorbed molecule will affect the amplitude of SFG (eq 3). Figure 4 illustrates the Euler angles
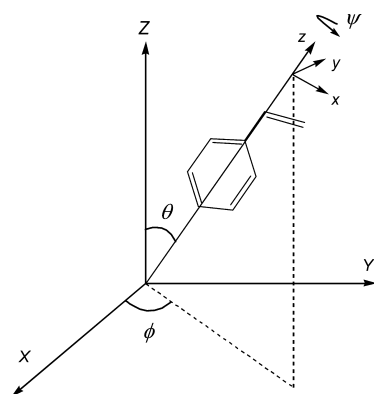
Figure 4. Definition of Cartesian coordinates and Euler angles (ϕ, θ, ψ) connecting the laboratory frame *XYZ* and the molecular coordinates *xyz* of styrene monomer.

(ϕ, θ, ψ) connecting the laboratory frame *XYZ* and the molecular coordinates *xyz*. Assuming that the molecules have a random azimuthal distribution, the ϕ-related components are averaged out while (θ, ψ) parameters remain and determine the signal amplitude. Given the incident beam angles θ_{IR} = 54° and θ_{Vis} = 60° (corresponding to the settings applied in ref 10) and the output angle θ_{SFG} = 45° and the damping constant as 5 cm^{-1} for each mode, the simulated SFG spectra of a styrene monomer at selected tilt angles with different combinations of polarization are depicted in Figure 5. It shows that:

(1) The ppp signals had similar amplitudes to the ssp ones, whereas the sps amplitudes were apparently one-order smaller.

(2) The most obvious features in the ssp spectrum at (0°, 0°) were ν_2 and ν_{7a} peaks. The intensity of the former gradually decreased, whereas the latter first increased and then decreased, as θ increases up to 90°. The influence from ψ was minor. All other modes were insignificant.

(3) Peaks of ν_{7a} and ν_{7b} showed up in the sps spectra, but both were weak as described above.

(4) In the ppp spectra, phenyl ν_{7a} and ν_2 as well as vinyl ν_9 and ν_{11} peaks dominated, whereas phenyl ν_{20a} made a minor contribution.

(5) All signals were expected to diminish as the molecule "lay down" to the *XY* plane because these high-frequency modes are all in the plane of the aromatic ring. This trend could be seen in the Figure as the tilt angles approach (90°, 90°).

Notice that there was not any real "surface" and the molecule was indeed free in this case. This condition could be similar to a weak adsorption system or the topmost adsorbate layer, where the adsorbate−air interaction is much more important than the influence from the substrate surface. Comparing our simulated spectra with previous experimental reports, we found that the orientation (θ, ψ) = (60°, 45°) approximated the ssp and sps signals obtained by Briggman et al. (cf. figure 3 in ref 9), which was consistent with their data analysis. The (20°, 0°) orientation roughly fit the ssp spectra at the PS/air interface reported by Gautam et al. (cf. figure 2 in ref 8) and gave a good fitting to ssp and ppp spectra shown by Chen et al. (cf. figure 2 in ref 10), in agreement to their suggestion that phenyl groups stand closely to the surface normal. The distribution window of tilt angles in each case was rather narrow, for example, in the range of ±10°, supposed in those reports and supported by our simulation, indicating that all phenyl units have a regular alignment. The large discrepancy in tilt angles between different reports might be a result of different adsorbate thickness and substrate material.

We have also calculated properties of a single ethylbenzene molecule because the C−C backbone is single-bonded rather than double-bonded in a real polymer. However, signals from vibrational modes of the free ethyl group, especially CH$_3$ modes at ~2920 and ~2990 cm^{-1}, which should be rare in a real polymer, dominated the SFG spectra, as depicted in Figure 6. It turns out that polymer-like alkyl modes rather than free ethyl or free vinyl modes are necessary in simulating spectra of the real polymer. Moreover, when a styrene dimer or oligomer could give a chemically correct C−C backbone, its rotation prevented us from describing the orientation by using simple (θ, ψ) angles. Therefore, a real surface was added to our model systems to select most possible conformers as shown in the next section.

2. Spectra of Ethylbenzene and Styrene Oligomers Adsorbed on Graphene. *Stable Conformers.* Several optimized geometric configurations of ethylbenzene and styrene oligomers adsorbed on a graphene sheet are depicted in Figure 7, where the stabilization energies are shown as well. The adsorption was quite weak but not negligible, ranging from 0.6 to 1.7 kcal/mol for the most stable structures calculated by
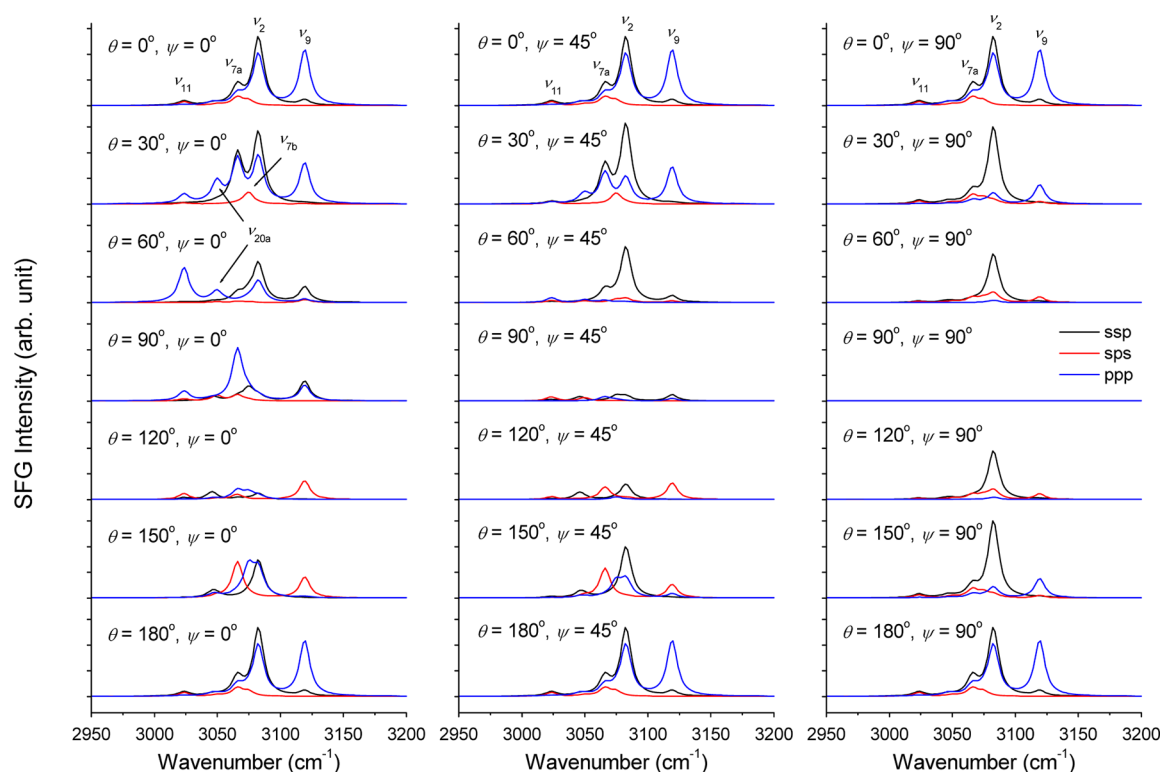
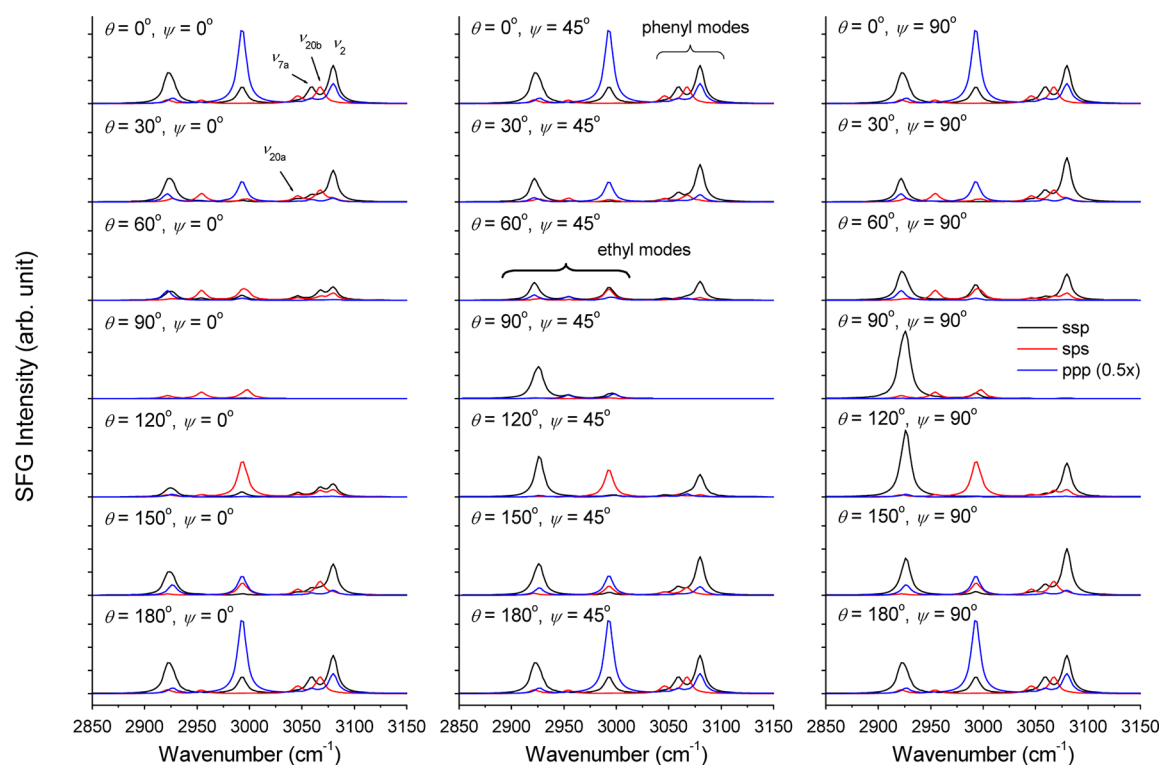**Figure 5.** Simulated SFG spectra of styrene monomer at selected tilt angles (θ, ψ).

Figure 6. Simulated SFG spectra of ethylbenzene at selected tilt angles (θ, ψ).

B3LYP/6-31G(d). The shortest carbon-to-carbon distance between the adsorbate and the surface was ~4 Å in all cases. However, it might be concerned whether the B3LYP functional could properly describe the long-range interaction. We therefore tested our model systems with M06 and M06-HF functionals, which included long-range exchange-correla-

tion.[23,24] It gave slight increases in adsorption energies, for example, from 1.2 kcal/mol with B3LYP to 2.7 kcal/mol with M06 and M06-HF for the ethylbenzene−graphene system (a) (i.e., etb(a) in Figure 7). In the meantime, the conformation, vibrational frequencies, and polarizability changed insignif-
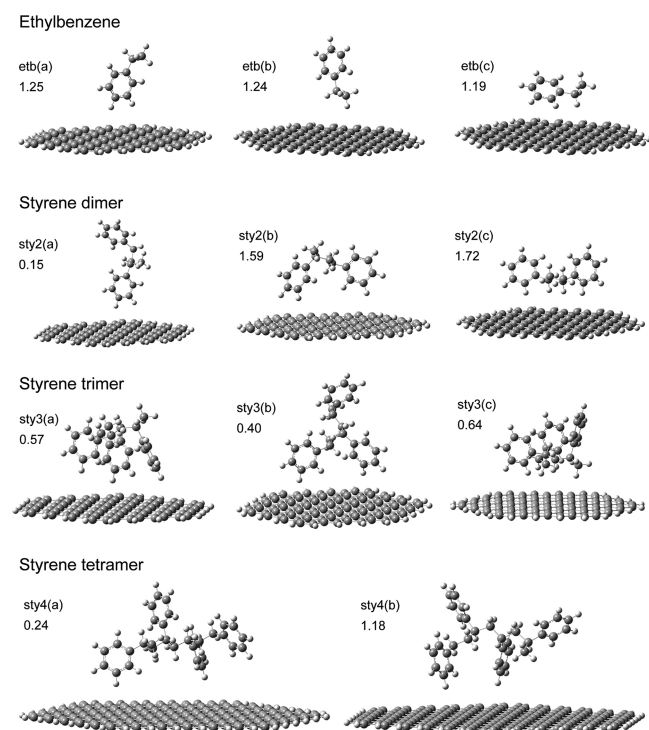
Figure 7. Optimized structures and stabilization energies (in kcal/mol) of ethylbenzene–graphene and styrene oligomer–graphene systems calculated by B3LYP/6-31G(d).

icantly. The results showed that the B3LYP functional, a relatively cheaper choice, was applicable in our systems.

Despite of the weak interaction, the phenyl planes always tended to stand perpendicular (whether upward or downward) to the graphene surface rather than to lay parallel to it. The angle between a single phenyl plane and the surface normal was typically <20° and seldom exceeded 40° in these optimized structures. It should be noticed that in our current simulations there was only one layer of adsorbate and hence it possessed both styrene/air and styrene/graphene interfaces. This condition was different from previous experimental reports where the two interfaces were well-separated by the thickness of the PS layer.

As the number of polymerized units increases, one would expect a gradual enhancement of stabilization or a more regular orientation of the side groups. In the current study, however, there was not any obvious tendency in either adsorption energy or ordered arrangement. The major reason might be that the number of units (only up to four here) was not enough to keep a regular conformation. A certain threshold for an ordered polymer structure should exist, although the number could be large, so it requires much more computational resources.

SFG Spectra. The IR and Raman spectra of ethylbenzene–graphene, styrene dimer–graphene, and styrene trimer–graphene systems had small differences in the C–H stretching region compared with those of sole adsorbate molecules. This was expected because the adsorption interaction was quite weak so that the vibrational modes of the adsorbate were slightly influenced. The SFG spectra were determined by the orientation of the adsorbate and hence were considerably affected by the surface. Figure 8 shows simulated SFG spectra of selected stable conformers under different combinations of beam polarization (ssp, sps, and ppp). It could be seen that peak positions of all alkyl C–H stretching modes (<3010 cm^{-1}) and phenyl C–H stretching modes (>3040 cm^{-1}) were essentially independent of adsorption orientations, whereas the intensities, as expected, were significantly diverse between conformers. The only trend one could see was that ppp signals were the most intense, whereas the sps ones are about one-
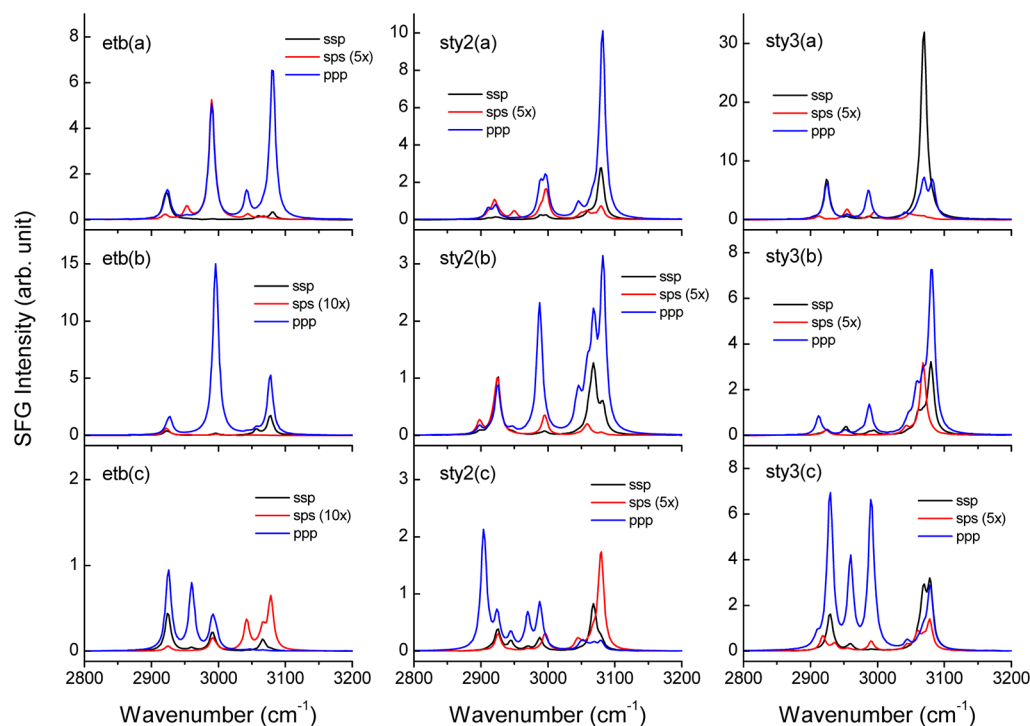

Figure 8. Simulated SFG spectra of ethylbenzene–graphene and styrene oligomer–graphene systems. The corresponding conformers are shown in Figure 7.

order smaller in most cases. There was no other regulation, as discussed on stabilization energy and conformation, attributed to too few styrene units so that we could hardly make a meaningful comparison with experimental spectra. A more extensive study on longer polymerized chains is in progress to investigate the regulations on energies, structures, as well as SFG spectra.

V. CONCLUSIONS

In this work, we have investigated the SFG properties of the styrene—graphene adsorption system with a theoretical approach. As a first step, the dipole derivatives and polarizability derivatives of C—H stretching vibrational modes of a single styrene molecule were computed. It was followed by calculation of second-order susceptibility and construction of orientation-dependent SFG spectra by varying tilt angles with respect to a virtual surface. The results supported the idea that all phenyl units might have a regular alignment found in experimental reports on PS adsorbed on a surface. In the next step, styrene monomer and its single-bond analogue, ethylbenzene, as well as styrene oligomers up to four units were put above a graphene sheet. Geometric optimization showed that phenyl groups tend to stand perpendicular rather than lay parallel to the surface. However, there was a large deviation on shapes and orientations of stable conformers so that no obvious trend in either adsorption energies or SFG spectra could be observed. This was attributed to the number of units that was too few; therefore, an elongation of the oligomer chain is required to generate a more regular polymer-like structure. To our knowledge, this work is the first systematic theoretical study on the orientation and SFG spectra of styrene oligomers adsorbed on a flat surface. Although it is somewhat far away from simulating the PS case that has been measured in experiments, this study provides a logical insight into the problem of how the polymer units align upon a surface.

■ AUTHOR INFORMATION

Corresponding Author
*E-mail: ethene@gate.sinica.edu.tw.

Notes
The authors declare no competing financial interest.

■ ACKNOWLEDGMENTS

■ REFERENCES

(1) Hayashi, M.; Lin, S. H. Molecular Theory of Sum-Frequency Generations and Its Applications to Study Molecular Chirality. In *Advances in Multi-Photon Processes and Spectroscopy*; Lin, S. H., Villaeys, A. A., Fujimura, Y., Eds; World Scientific: Singapore, 2004; Vol. *16*, pp 307−422.

(2) Wei, X.; Miranda, P. B.; Zhang, C.; Shen, Y. R. Sum-Frequency Spectroscopic Studies of Ice Interfaces. *Phys. Rev. B* **2002**, *66*, 085401.

(3) Moad, A. J.; Simpson, G. J. A Unified Treatment of Selection Rules and Symmetry Relations for Sum-Frequency and Second Harmonic Spectroscopies. *J. Phys. Chem. B* **2004**, *108*, 3548−3562.

(4) Belkin, M. A.; Shen, Y. R. Non-Linear Optical Spectroscopy as a Novel Probe for Molecular Chirality. *Intl. Rev. Phys. Chem* **2005**, *24*, 257−299.

(5) Du, Q.; Superfine, R.; Freysz, E.; Shen, Y. R. Vibrational Spectroscopy of Water at the Vapor/Water Interface. *Phys. Rev. Lett.* **1993**, *70*, 2313−2316.

(6) Shen, Y. R.; Ostroverkhov, V. Sum-Frequency Vibrational Spectroscopy on Water Interfaces: Polar Orientation of Water Molecules at Interfaces. *Chem. Rev.* **2006**, *106*, 1140−1154.

(7) Tian, C.-S.; Shen, Y. R. Isotopic Dilution Study of the Water/Vapor Interface by Phase-Sensitive Sum-Frequency Vibrational Spectroscopy. *J. Am. Chem. Soc.* **2009**, *131*, 2790−2791.

(8) Gautam, K. S.; Schwab, A. D.; Dhinojwala, A.; Zhang, D.; Dougal, S. M.; Yeganeh, M. S. Molecular Structure of Polystyrene at Air/Polymer and Solid/Polymer Interfaces. *Phys. Rev. Lett.* **2000**, *85*, 3854−3857.

(9) Briggman, K. A.; Stephenson, J. C.; Wallace, W. E.; Richter, L. J. Absolute Molecular Orientational Distribution of the Polystyrene Surface. *J. Phys. Chem. B* **2001**, *105*, 2785−2791.

(10) Chen, C.; Wang, J.; Woodcock, S. E.; Chen, Z. Surface Morphology and Molecular Chemical Structure of Poly(*n*-butyl methacrylate)/Polystyrene Blend Studied by Atomic Force Microscopy (AFM) and Sum-Frequency Generation (SFG) Vibrational Spectroscopy. *Langmuir* **2002**, *18*, 1302−1309.

(11) Guthmuller, J.; Cecchet, F.; Lis, D.; Caudano, Y.; Mani, A. A.; Thiry, P. A.; Peremans, A. Champagne, B. Theoretical Simulation of Vibrational Sum-Frequency Generation Spectra from Density Functional Theory: Application to *p*-Nitrothiophenol and 2,4-Dinitroaniline. *ChemPhysChem* **2009**, *10*, 2132−2142.

(12) Perry, J. M.; Moad, A. J.; Begue, N. J.; Wampler, R. D.; Simpson, G. J. Electronic and Vibrational Second-Order Nonlinear Optical Properties of Protein Secondary Structural Motifs. *J. Phys. Chem. B* **2005**, *109*, 20009−20026.

(13) Han, H.-L.; Tian, C.-S.; Shen, Y. R. **2012**, to be submitted for publication.

(14) Frisch, M. J.; Trucks, G. W.; Schlegel, H. B.; Scuseria, G. E.; Robb, M. A.; Cheeseman, J. R.; Scalmani, G.; Barone, V.; Mennucci, B.; Petersson, G. A.; et al. *Gaussian 09*, revision A.02; Gaussian, Inc.: Wallingford, CT, 2009.

(15) Irikura, K. K.; Johnson, R. D., III; Kacker, R. N. Uncertainties in Scaling Factors for ab Initio Vibrational Frequencies. *J. Phys. Chem. A* **2005**, *109*, 8430−8437.

(16) National Institute of Standards and Technology. Computational Chemistry Comparison and Benchmark DataBase. http://cccbdb.nist.gov/ (accessed Oct 10, 2012).

(17) National Institute of Standards and Technology. NIST Chemistry WebBook. http://webbook.nist.gov/ (accessed Oct 10, 2012).

(18) Sears, W. M.; Hunt, J. L.; Stevens, J. R. Raman Scattering from Polymerizing Styrene. I. Vibrational Mode Analysis. *J. Chem. Phys.* **1981**, *75*, 1589−1598.

(19) Varsányi, G. *Vibrational Spectra of Benzene Derivatives*; Academic Press: New York, 1969.

(20) Duffy, D. C.; Davies, P. B.; Bain, C. D. Surface Vibrational Spectroscopy of Organic Counterions Bound to a Surfactant Monolayer. *J. Phys. Chem.* **1995**, *99*, 15241−15246.

(21) National Institute of Advanced Industrial Science and Technology, Japan. Spectral Database for Organic Compounds SDBS. http://riodb01.ibase.aist.go.jp/sdbs/ (accessed Oct 10, 2012).

(22) Condirston, D. A.; Laposa, J. D. Vibrational Spectra of Styrene-H8, -D3, -D5, and -D8. *J. Mol. Spectrosc.* **1976**, *63*, 466−477.

(23) Zhao, Y.; Truhlar, D. G. Density Functional for Spectroscopy: No Long-Range Self-Interaction Error, Good Performance for Rydberg and Charge-Transfer States, and Better Performance on Average than B3LYP for Ground States. *J. Phys. Chem. A* **2006**, *110*, 13126−13130.

(24) Zhao, Y.; Truhlar, D. G. The M06 Suite of Density Functionals for Main Group Thermochemistry, Thermochemical Kinetics, Noncovalent Interactions, Excited States, and Transition Elements: Two New Functionals and Systematic Testing of Four M06-Class Functionals and 12 Other Functionals. *Theor. Chem. Acc.* **2008**, *120*, 215−241.